MICROWAVE ELECTROMAGNETICS

COMPARISON OF EXACT AND APPROXIMATE ABSORBING CONDITIONS FOR INITIAL BOUNDARY VALUE PROBLEMS OF THE ELECTROMAGNETIC THEORY OF GRATINGS

V.L. Pazynin,[1] S.S. Sautbekov,[2] K.Yu. Sirenko,[1]
Yu.K. Sirenko,[1],♦ A.A. Vertiy,[3] & N.P. Yashina[1]

[1]*O.Ya. Usikov Institute for Radio Physics and Electronics, National Academy of Sciences of Ukraine, 12 Academician Proskura St., Kharkiv 61085, Ukraine*

[2]*Al-Farabi Kazakh National University, 71 Al-Farabi Ave., Almaty 050040, Republic of Kazakhstan*

[3]*Ukrainian Institute for Scientific and Technical Expertise and Information, 180 Antovicha St., Kyiv 36150, Ukraine*

♦*Address all correspondence to: Yu.K. Sirenko, E-mail: yks2002sky@gmail.com*

The paper presents comparison of several exact and approximate absorbing conditions, which are used to truncate computation domains of open (unbounded) initial boundary value problems of the electromagnetic theory of gratings. This comparison allows to judge the reliability and efficiency of absorbing conditions widely used in computational practice. The paper demonstrates that in cases, when resonant wave scattering is possible, only exact absorbing conditions allow to preserve the stability and convergence of computational schemes, and to provide a required level of accuracy in calculating the diffraction characteristics of open periodic resonators.

KEY WORDS: *initial boundary value problems, computational electromagnetic methods, method of exact absorbing conditions, periodic gratings, stability and convergence of computational schemes, resonance domain*

1. INTRODUCTION

Many real-world devices or processes are described with open initial-boundary value problems, i.e., problems with unbounded domains of interest. To be able to solve such

problems numerically, one must truncate an unbounded domain of interest to a bounded computation domain. Correct and efficient limitation of computation domains is one of the most important and difficult issues in modern computational electrodynamics [1]. A significant progress in solving this issueis associated with development of the following domain truncation techniques: (i) Absorbing boundary conditions (ABCs), which mimic unbounded external regions with certain assumptions and simplifications [2–5]; (ii) Perfectly matched layers (PMLs), which wrap computation domain with special absorbing materials [6–8]; (iii) Exact absorbing conditions (EACs), which mimic unbounded external regions using mathematically rigorous boundary conditions [9–15]. All domain truncation techniques are aimed to turn open problems (problems with unbounded domains of interest) into closed ones (problems with bounded computation domains). But only EACs allow an equivalent, mathematically rigorous replacement of original open problem with a closed one. There are no general proofs of correctness and efficiency for each of the domain truncation techniques, thus additional arguments should be taken into account when choosing one for a particular physical or applied problem. Such arguments could be obtained from the results of a comprehensive comparative analysis of different domain truncation techniques, which are presented in this paper.

This topic was briefly touched in [10,12,13,15–17]. In this paper, it is further developed via studies of solutions to initial boundary value problems of the electrodynamic theory of gratings [14,15].

2. PROBLEM FORMULATION

The physically and mathematically correct formulation of a closed initial-boundary value problem, which describes transformations of the electromagnetic field by a grating with periodicity in one dimension (Fig. 1), has the following form [14,15]:

$$
\begin{cases}
\left[-\varepsilon(g)\partial_t^2 - \sigma(g)\eta_0\partial_t + \partial_y^2 + \partial_z^2 \right] U(g,t) = 0; \quad g \in \Omega_{\text{int}}, \quad t > 0 \\
U(g,0) = 0, \quad \partial_t U(g,t)\big|_{t=0} = 0; \quad g = \{y,z\} \in \bar{\Omega}_{\text{int}} \\
\vec{E}_{tg}(g,t) \text{ and } \vec{H}_{tg}(g,t) \text{ are continuous when crossing } \Sigma^{\varepsilon,\sigma}, \quad \vec{E}_{tg}(g,t)\big|_{g\in\Sigma} = 0, \\
U(l,z,t) = \mathrm{e}^{2\pi i \Phi} U(0,z,t), \quad \partial_y U(l,z,t) = \mathrm{e}^{2\pi i \Phi}\partial_y U(0,z,t) \text{ for } |z| < L, \\
D_+\left[U(g,t) - U_p^i(g,t) \right]\big|_{g\in\Gamma_+} = 0, \quad D_-\left[U(g,t) \right]\big|_{g\in\Gamma_-} = 0; \quad t \geq 0.
\end{cases}
\tag{1}
$$

Here, $U(g,t) = E_x(g,t)$ in the case of E-polarization ($\partial_x \equiv 0$, $E_y = E_z = H_x = 0$), and $U(g,t) = H_x(g,t)$ in the case of H-polarization ($\partial_x \equiv 0$, $H_y = H_z = E_x = 0$); $\vec{E}(g,t) = \{E_x, E_y, E_z\}$ and $\vec{H}(g,t) = \{H_x, H_y, H_z\}$ are the electric and magnetic field

vectors; $\{x, y, z\}$ are the Cartesian coordinates; the piecewise-constant functions $\sigma(g) \geq 0$ and $\varepsilon(g) \geq 1$ are the specific conductivity and the relative permittivity of dielectric elements; $\eta_0 = (\mu_0/\varepsilon_0)^{1/2}$ is the impedance of free space; ε_0 and μ_0 are the electric and magnetic vacuum constants; Φ is a real-valued parameter introduced by the constant wavenumber approach to the oblique incidence treatment [1,14,15], $|\Phi| \leq 0.5$. The surfaces of perfect electric conductors (PECs) Σ and discontinuities in material parameters $\Sigma^{\varepsilon,\sigma}$ are assumed to be sufficiently smooth.
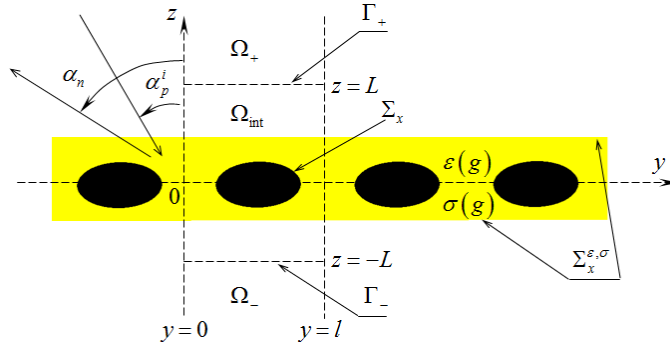

FIG. 1: 2-D grating with periodicity in one dimension

The computation domain Ω_{int} of the problem (1) is a part of the Floquet channel $\mathrm{R} = \{g = \{y, z\} : 0 < y < l, |z| < \infty\}$, bounded by the PEC surfaces and the virtual boundaries $\Gamma_{\pm}$. On these boundaries the following conditions are enforced: $D_+\left[U(g,t) - U_p^i(g,t)\right]\Big|_{g \in \Gamma_+} = 0, \qquad D_-\left[U(g,t)\right]\Big|_{g \in \Gamma_-} = 0.$ They "absorb" waves propagating towards reflection ($\Omega_+ = \{g \in \mathrm{R} : z > L\}$) and transition ($\Omega_- = \{g \in \mathrm{R} : z < -L\}$) zones of a grating. These waves are set by

$$U_+^s(g,t) = U(g,t) - U_p^i(g,t) = \sum_{n=-\infty}^{\infty} u_{n+}(z,t)\mu_n(y); \quad g \in \overline{\Omega}_+,$$

$$U_-^s(g,t) = U(g,t) = \sum_{n=-\infty}^{\infty} u_{n-}(z,t)\mu_n(y); \quad g \in \overline{\Omega}_-.$$

(2)

Here, $\{\mu_n(y)\}_{n=-\infty}^{\infty}$ is complete (on interval $0 < y < l$), orthonormal system of functions $\mu_n(y) = l^{-1/2}\exp(i\Phi_n y)$, $\Phi_n = (n + \Phi)2\pi/l$, and $U_p^i(g,t) = v_{p+}(z,t)\mu_p(y)$, $g \in \overline{\Omega}_+$ is an incident pulse which excites a periodic structure.

In the frequency domain, a periodic structure is characterized by reflection and transmission coefficients, $R_{np}(k)$ and $T_{np}(k)$, given by the following formulas:

$$R_{np}(k) = \frac{\tilde{u}_{n+}(L,k)}{\tilde{v}_{p+}(L,k)}, \quad T_{np}(k) = \frac{\tilde{u}_{n-}(-L,k)}{\tilde{v}_{p+}(L,k)}. \tag{3}$$

Here, ~ denotes application of the integral transform $\tilde{f}(k) = \int_0^T f(t)\exp(ikt)dt$, $k = 2\pi/\lambda$ is a wavenumber (frequency parameter), λ is a wavelength, T is a duration of simulation. $R_{np}(k)$ and $T_{np}(k)$ are the amplitudes of plane homogeneous and inhomogeneous waves (harmonics) appearing in the reflection and transmission zones of a grating when it is excited by a plane wave $\tilde{U}_p^i(g,k) = \exp[-i\Gamma_p(z-L)]\mu_p(y)$, $g \in \bar{\Omega}_+$, $\Gamma_p = (k^2 - \Phi_p^2)^{1/2}$, $\mathrm{Re}\,\Gamma_p \geq 0$, $\mathrm{Im}\,\Gamma_p \geq 0$. They satisfy the relations

$$\sum_{n=-\infty}^{\infty}\left[\left|R_{np}\right|^2 + \left|T_{np}\right|^2\right]\mathrm{Re}\,\Gamma_n = \mathrm{Re}\,\Gamma_p + 2\,\mathrm{Im}\,R_{pp}\,\mathrm{Im}\,\Gamma_p - \frac{k^2}{\beta_0}W_1,$$

$$\sum_{n=-\infty}^{\infty}\left[\left|R_{np}\right|^2 + \left|T_{np}\right|^2\right]\mathrm{Im}\,\Gamma_n = \mathrm{Im}\,\Gamma_p - 2\,\mathrm{Im}\,R_{pp}\,\mathrm{Re}\,\Gamma_p - \frac{k^2}{\beta_0}W_2, \tag{4}$$

which are obtained from analytical form of the energy conservation law. Here, $W_1 = \frac{\eta_0\varepsilon_0}{k}\int_{\Omega_{\mathrm{int}}}\sigma(g)\left|\tilde{\vec{E}}(g,k)\right|^2 dg$ and $W_2 = \pm\int_{\Omega_{\mathrm{int}}}\left[\mu_0\left|\tilde{\vec{H}}(g,k)\right|^2 - \varepsilon(g)\varepsilon_0\left|\tilde{\vec{E}}(g,k)\right|^2\right]dg$; the plus sign and $\beta_0 = \varepsilon_0$ should be used in the case of E-polarization, and the minus sign and $\beta_0 = \mu_0$ should be used in the case of H-polarization.

For $\mathrm{Re}\,\Gamma_p > 0$, the angle $\alpha_p^i = \arcsin(\Phi_p/k)$ is the incidence angle of the wave $\tilde{U}_p^i(g,k)$ coming onto a grating. Every harmonic $\tilde{U}_{n\pm}^s(g,k)$ of the fields

$$\tilde{U}_+^s(g,k) = \sum_{n=-\infty}^{\infty}\tilde{U}_{n+}^s(g,k) = \sum_{n=-\infty}^{\infty}R_{np}\exp[i\Gamma_n(z-L)]\mu_n(y); \quad g \in \Omega_+,$$

$$\tilde{U}_-^s(g,k) = \sum_{n=-\infty}^{\infty}\tilde{U}_{n-}^s(g,k) = \sum_{n=-\infty}^{\infty}T_{np}\exp[-i\Gamma_n(z+L)]\mu_n(y); \quad g \in \Omega_-, \tag{5}$$

with $\mathrm{Im}\,\Gamma_n = 0$ and $\mathrm{Re}\,\Gamma_n > 0$, is an homogeneous plane wave propagating away from a grating at the angle $\alpha_n = -\arcsin(\Phi_n/k)$ into the reflection zone ($z > L$), and at the angle $\alpha_n = \pi + \arcsin(\Phi_n/k)$ into the transmission zone ($z < -L$). All angles are measured anticlockwise from the z-axis in the plane $y0z$ (Fig. 1). It is obvious that the propagation direction of each homogeneous harmonic of the secondary field

depends on its number n, as well as on the values of k and α_p^i. The angle between propagation directions of the primary and the ($-m$)-th reflected plane waves is $2\alpha = \alpha_p^i - \alpha_{-m}$, it is obtained from the equation $kl\sin(\alpha_p^i - \alpha)\cos\alpha = \pi(p+m)$. At $\alpha = 0$, the corresponding harmonic propagates countercurrent to an incident wave, it is called the autocollimation phenomenon. According to (4), the values

$$W_{\text{abs}}(k) = \frac{k^2}{\beta_0 |\Gamma_p|} W_1, \quad W_{np}^R(k) = |R_{np}|^2 \frac{\operatorname{Re}\Gamma_n}{|\Gamma_p|}, \quad W_{np}^T(k) = |T_{np}|^2 \frac{\operatorname{Re}\Gamma_n}{|\Gamma_p|} \tag{6}$$

determine the relative part of energy that is absorbed or redirected by a grating into reflected and transmitted harmonics.

3. ABSORBING CONDITIONS

From a fairly wide range of known exact and approximate absorbing conditions which could be used in the problem (1) [15,17], the following were chosen for the comparison:
(i) Nonlocal EAC [12,18]

$$U_\pm^s(y, \pm L, t) =$$
$$= \mp \sum_{n=-\infty}^{\infty} \left\{ \int_0^t J_0\left[\Phi_n(t-\tau)\right] \left[\int_0^l \partial_z U_\pm^s(\tilde{y}, \tilde{z}, \tau)\Big|_{\tilde{z}=\pm L} \mu_n^*(\tilde{y})d\tilde{y} \right] d\tau \right\} \mu_n(y); \tag{7}$$

$0 \le y \le l, \quad t \ge 0, \quad J_0(\ldots)$ is the Bessel function.

Its accuracy is controlled by a number of harmonics accounted in (7), N.
(ii) Local EAC [12,18]

$$U_\pm^s(y, \pm L, t) = -\frac{1}{2\pi} \int_{-\pi}^{\pi} W_\pm(y, t, \varphi)d\varphi; \quad 0 \le y \le l, \quad t \ge 0$$

$$\begin{cases} \left[\partial_t - \sin\varphi\partial_y\right] W_\pm(y, t, \varphi) = \pm\partial_z U_\pm^s(y, z, t)\Big|_{z=\pm L}; \quad 0 < y < l, \quad t > 0 \\ W_\pm(y, 0, \varphi) = \partial_t W_\pm(y, t, \varphi)\Big|_{t=0} = 0; \quad 0 \le y \le l \\ W_\pm(d, t, \varphi) = e^{i2\pi\Phi} W_\pm(0, t, \varphi), \\ \partial_y W_\pm(d, t, \varphi) = e^{i2\pi\Phi} \partial_y W_\pm(0, t, \varphi); \quad t \ge 0. \end{cases} \tag{8}$$

Its accuracy is controlled by M, which is a number of steps the interval $\varphi \le |\pi|$ is divided for numerical integration in (8).

(iii) ABC of second-order approximation [1]

$$\left[\pm\partial_t\partial_z - \partial_t^2 + 0.5\partial_y^2\right]U_\pm^s(y,z,t)\Big|_{z=\pm L} = 0; \quad 0 \le y \le l, \quad t \ge 0. \tag{9}$$

(iv) ABC of third-order approximation [1]

$$\left[\mp\partial_t^2\partial_z \pm 0.25\partial_y^2\partial_z - \partial_t^3 + 0.75\partial_t\partial_y^2\right]U_\pm^s(y,z,t)\Big|_{z=\pm L} = 0; \quad 0 \le y \le l, \quad t \ge 0. \tag{10}$$

(v) PML. Its accuracy is controlled by thickness d, index n of absorption growth rate $\sigma(z) = \sigma_{max}\left[(|z|-L)/d\right]^n$, and theoretical reflection coefficient at normal incidence R [1].

4. SIMPLE TEST

For the first test, the grating profile is a PEC plane $z = 0$, $l = 2\pi$, $L = \pi$. H-polarized wave, which is set by

$$U_0^i(g,t):$$

$$\Phi = 0.2 \quad \text{and} \quad v_{0+}(L,t) = 4\frac{\sin\left[\Delta k\left(t-\tilde{T}\right)\right]}{\left(t-\tilde{T}\right)}\cos\left[\tilde{k}\left(t-\tilde{T}\right)\right]\chi\left(\overline{T}-t\right) = F_1(t); \tag{11}$$

$$\tilde{k} = 0.45, \quad \Delta k = 0.1, \quad \tilde{T} = 250, \quad \overline{T} = 500.$$

falls on this grating. Here, $\chi(...)$ is the Heaviside step function, $\tilde{k}$, $\tilde{T}$, and $\overline{T}$ are central frequency, delay time and width of the pulse $F_1(t)$. Parameter Δk specifies the frequency band $\tilde{k} - \Delta k \le k \le \tilde{k} + \Delta k$ of the pulse. In our case, it is $0.35 \le k \le 0.55$. These values of k correspond to the angles $21.3° \le \alpha_0^i \le 34.8°$ of arrival of the plane waves $\tilde{U}_0^i(g,k) = \exp\left[-i\Gamma_0(z-L)\right]\mu_0(y)$. The structure is not transformative, and therefore only one harmonic $\tilde{U}_{0+}^s(g,k) = R_{00}\exp\left[i\Gamma_0(z-L)\right]\mu_0(y)$ exists in the reflection zone. The exact value of corresponding reflection coefficient is $R_{00}(k) = \exp(i2\pi\Gamma_0)$.

The standard FDTD method [1] is used for numerical tests in this paper. Its approximation error is $O(\overline{h}^2)$, where $\overline{h}$ is space step, $\overline{l}$ denotes time step. For the first test, they are set as $\overline{h} = 0.031416$, $\overline{l} = 0.015$; the computation domain is meshed with 200 cells in both y and z directions; the number of time steps is 65 000, which

corresponds to the duration of computation $T = 975$; the number of harmonics in nonlocal EAC (i) is $N = 5$; the number of integration steps in local EAC (ii) is $M = 200$; PML thickness is $d = 32\bar{h}$, PML absorption has a quadratic profile ($n = 2$), and $R = 10^{-4}$.

Figure 2 presents the relative errors of $|R_{00}(k)|$ and $\arg R_{00}(k)$ obtained using the absorbing conditions listed above. The smallest error is demonstrated by nonlocal EAC (i) and PML (v). The largest error is demonstrated by second-order ABC (iii). Surprisingly, in all cases, Rel Error $|R_{00}(k)|$ vanishes at the same point $k = 0.538$, suggesting that $\arg R_{00}(k) = \pi$. In all cases, the computational scheme is stable, amplitude tails of pulses $u_{0+}(L,t)$ are 5 to 7 orders of magnitude smaller than their main parts.
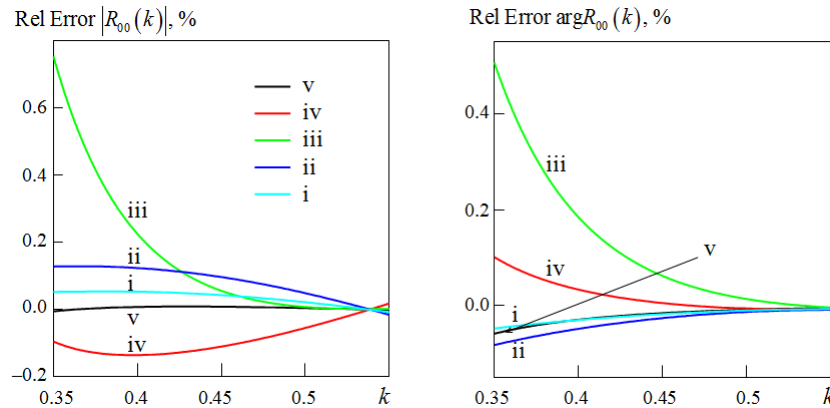

FIG. 2: Relative errors of $R_{00}(k)$ computed using conditions (i)–(v)

5. TEST WITH RESONANT SCATTERING

The second test is performed in usual for gratings conditions of possible resonant waves scattering. The periodic structure under study is 2-D photonic crystal with finite thickness ($h = 20\pi$, $l_y = l_z = l = 2\pi$), it is made of circular dielectric rods (radius $r = 0.38l$, $\varepsilon = 8.9$), Fig. 3. The structure is excited by the H-polarized wave (11). Within the band $0.35 \leq k \leq 0.55$, where the values $W_{00}^T(k)$ are calculated, only the fundamental harmonics ($n = 0$) propagate in the reflection and transmission zones of the periodic structure. The parameters of the computational scheme are following: $\bar{h} = 0.12566$ and $\bar{l} = 0.06$, the duration of computation $T = 7000$ (116 666 time

steps), $2L = h$. For absorbing conditions, the same settings were used as in the previous section.
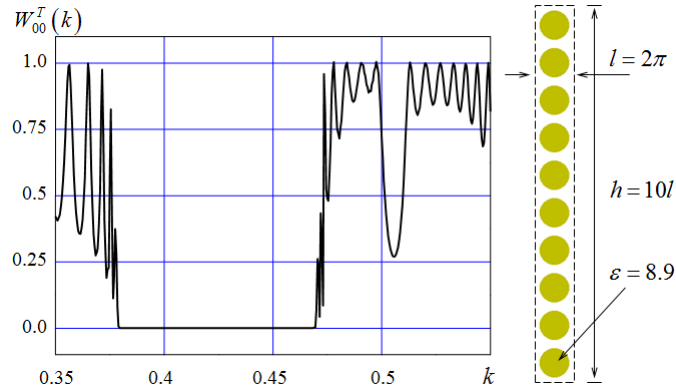

FIG. 3: Bandgap aned geometry of 2-D photonic crystal

   The only absorbing condition which provided a physically correct result was nonlocal EAC (i), Fig. 3. We use it below as a reference for calculating absolute errors Abs Error $W_{00}^T(k)$. In other experiments, the computational scheme has lost stability long before the end of observation time, Fig. 4. Under the loss of stability, here and further on, we mean an exponential increase of the field strength in the computation domain caused by the "transformation" of virtual boundaries into fictitious current sources. Numerical disaster occurs at different times and develops at different speeds. The speed is lowest with local EAC (ii). Surprisingly, the scheme with ABC (iii) turns out to be more stable than the schemes with ABC (iv) and PML (v).

   Reduction of the duration of computation to $T = 3000$ (50 000 time steps) prevents the collapse of computational schemes with local EAC (ii), ABC (iii) and PML (v), but errors levels remain unacceptable (Fig. 5) due to excitation of high-Q eigenmodes of the periodic structure. These modes correspond to complex eigenfrequencies with real parts within the band $0.35 \leq k \leq 0.55$ (it is occupied by the pulse $U_0^i(g, t)$) [19,20].

   The thing is that time-domain results $f(t)$ are converted correctly into frequency-domain results $\tilde{f}(k)$ (see the integral transform after (3)) only when the values $f(t)$ are sufficiently small for $t > T$, i.e., only when the field $U(g, t)$ decays fast enough at all points of the domain Ω_{int}. But the amplitude of high-Q free oscillations decreases very slow over time. For the same reason, the virtual boundaries $\Gamma_{\pm}$ with approximate absorbing conditions on them can "turn" into fictitious sources of the field. And this field's rapidly increasing intensity leads to a numerical catastrophe. Such virtual boundaries simply do not stand the test of a long "contact" with waves whose amplitude remains high for a long time.
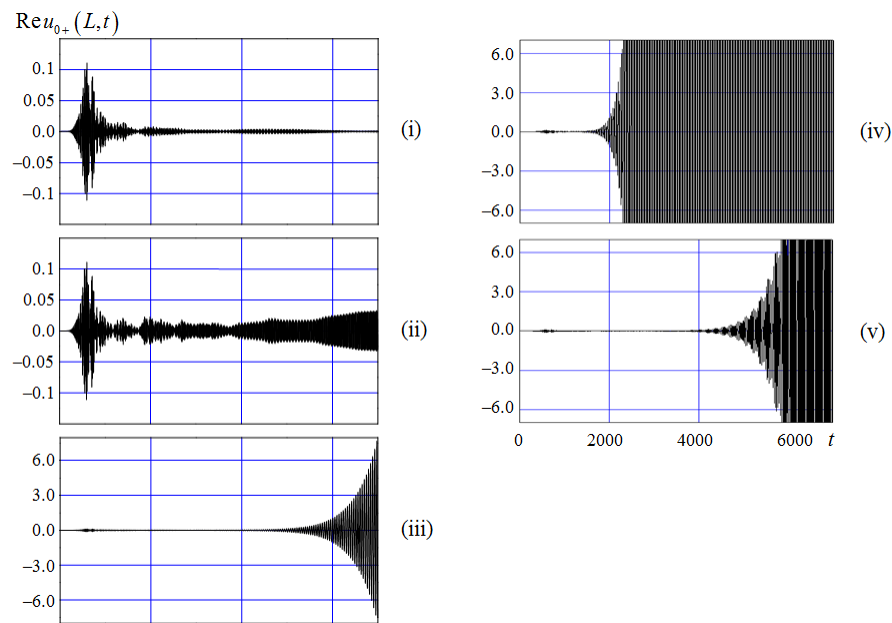
$\mathrm{Re}\, u_{0_+}(L,t)$

FIG. 4: Lack of stability in computations with conditions (i)–(v)
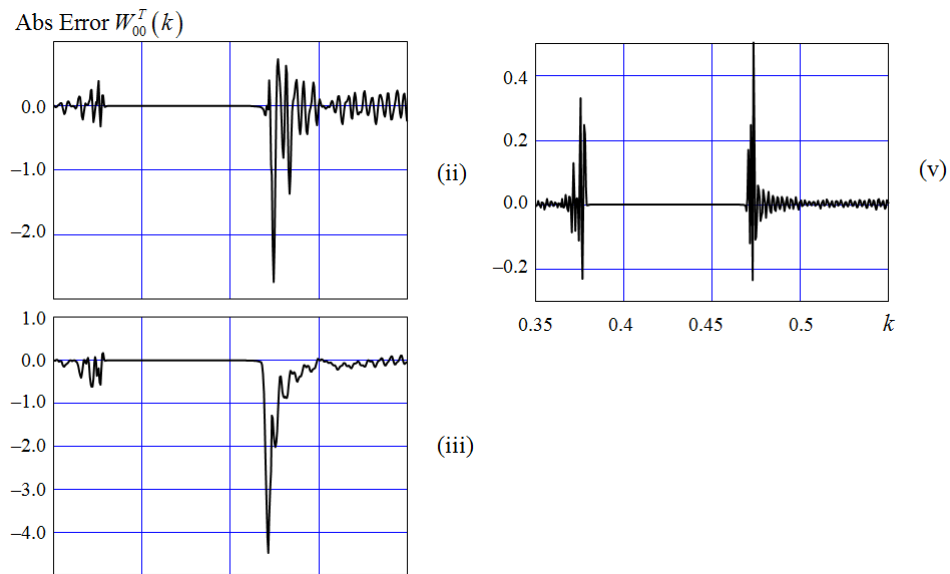
Abs Error $W_{00}^T(k)$

FIG. 5: Errors of $W_{00}^T(k)$ computed using conditions (ii), (iii), (v)

6. HARD TEST WITH SUPER-HIGH-FREQUENCY FREE OSCILLATIONS

Let us now consider the following problem: H-polarized pulse wave

$$U_0^i(g,t): \quad \Phi = 0 \quad \text{and} \quad v_{0+}(L,t) = F_1(t); \quad \tilde{k} = 0.5, \quad \Delta k = 0.45, \quad \tilde{T} = 100, \quad \overline{T} = 200$$

$$(12)$$

excites a lamellar semitransparent grating with a rather complex geometry (see Fig. 6: $l = 6.28314$, $h = 3.6018$, $\theta = 0.3$; $\varepsilon_1 = 2$ and $\varepsilon_2 = 4$ are the relative permittivities of the dielectric parts; thickness of the metal stripes is $2\overline{h}$). The pulse (12) covers the frequency band $0.05 \le k \le 0.95$, in which only principal harmonics propagate in the reflection and transmission zones of the grating without decay. From (4) and (6) follows that the relation $\eta(k) = 1 - W_{00}^T(k) - W_{00}^R(k) \equiv 0$ must hold. In contrast to the case considered above, the virtual boundaries $\Gamma_\pm$ are located far enough from the grating: $2L = 7.6038$. On these boundaries, the absorbing conditions (i)–(v) with the parameters $N = 5$, $M = 200$, $d = 32\overline{h}$, $n = 2$, $R = 10^{-4}$ are introduced. Discretization steps for the problem (1) are $\overline{h} = 0.02$ and $\overline{l} = 0.01$.
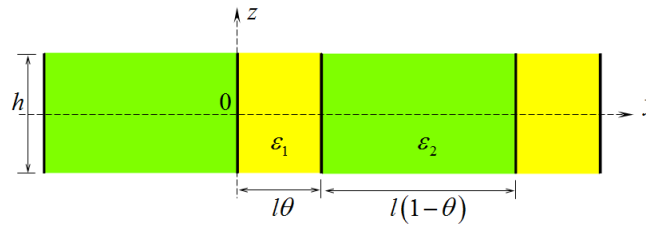

FIG. 6: Lamellar grating with a complex geometry

In the first series of computational experiments, the duration of computation was set to $T = 1000$, the analyzed frequency interval was discretized with the step of 10^{-4}. Only nonlocal EAC (i) provided the result with an acceptable accuracy, Figs. 7 and 8. The error is estimated from values of the function $\eta(k)$, which, in the case of lossless materials, must vanish when the problem is solved exactly(it follows from (4)). The solution obtained with nonlocal EAC (i) deviates from the exact solution only in a small neighborhood of the point $k = 0.823$, Fig. 7(a). This is the real part of the complex eigenfrequency $\overline{k} \approx 0.823 - i0.00038$ corresponding to an eigenmode. The pattern of its H_x-component at the moment of time $t = 930$ is presented in the upper fragment of Fig. 7(b). The quantities $\text{Re}\,\overline{k}$, $\text{Im}\,\overline{k}$, as well as the Q-factor of the eigenoscillation $Q = \text{Re}\,\overline{k}/2|\text{Im}\,\overline{k}| \approx 1080$, are determined from the data presented in the lower fragments of Fig. 7(a) (the spectral amplitudes $\tilde{U}(g_1, k, 250) =$ $= \int_{250}^T U(g_1, t)\exp(ikt)\,dt$ of the eigenfield $U(g_1, t)\chi(t - 250)$) and Fig. 7(b) (decrease of the field amplitude $U(g_1, t)\chi(t - 250)$) [13,18,20–22]. In the vicinity of the point

$k = 0.823$, the characteristics $W_{00}^T(k)$ and $W_{00}^R(k)$ are changing anomalously sharply (Fig. 7(a)), but their true behavior has yet to be determined.
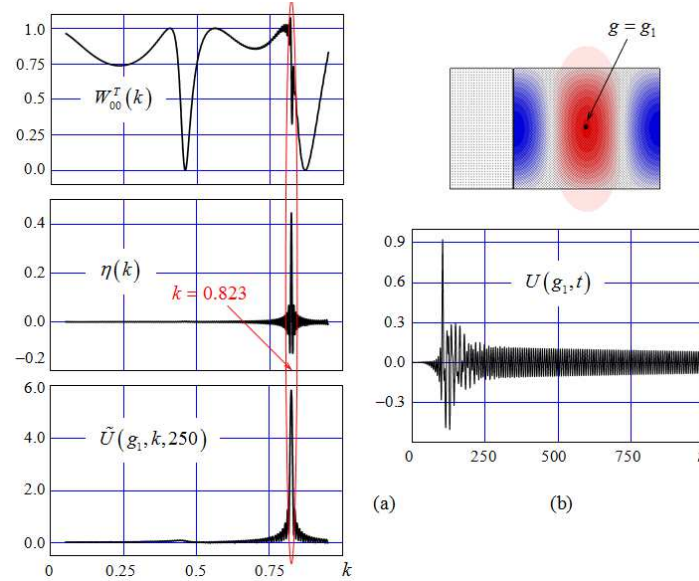

FIG. 7: Computation with condition (i): (a) Functions $W_{00}^T(k)$, $\eta(k)$, and $\tilde{U}(g_1, k, 250)$ within the frequency band $0.05 \leq k \leq 0.95$; (b) Characteristics of high-Q eigenmodes of the grating

The discrepancy characterizing the error in the energy conservation law is too large when conditions (ii)–(v) are used, and within frequency intervals where the total resonant reflection ($W_{00}^T(k) = 0$) of H-polarized plane waves occurs (Fig. 8). In the case of local EAC (ii), regular errors of the computational scheme are superimposed with the errors associated with a violation of stability for $t > 800$. For EACs (i) and (ii), and PML (v), we can try to improve the results changing the parameters N, M, d, n, and R. However, ABCs (iii) and (iv) are hopeless in this situation.

In the second series of computational experiments (Fig. 9), the duration of computation was set to $T = 5000$ (500 000 time steps), $N = 10$, $M = 2000$, $d = 64\bar{h}$, $n = 2$, and $R = 10^{-6}$. The most accurate solution was obtained using nonlocal EAC (i). Local EAC (ii) provides good results for durations of computation up to $T = 4000$, but the computational scheme begins to lose stability for $t > 4500$. PML (v) provides less accurate solution, but its error virtually do not change when T is varying from 2000 to 5000.
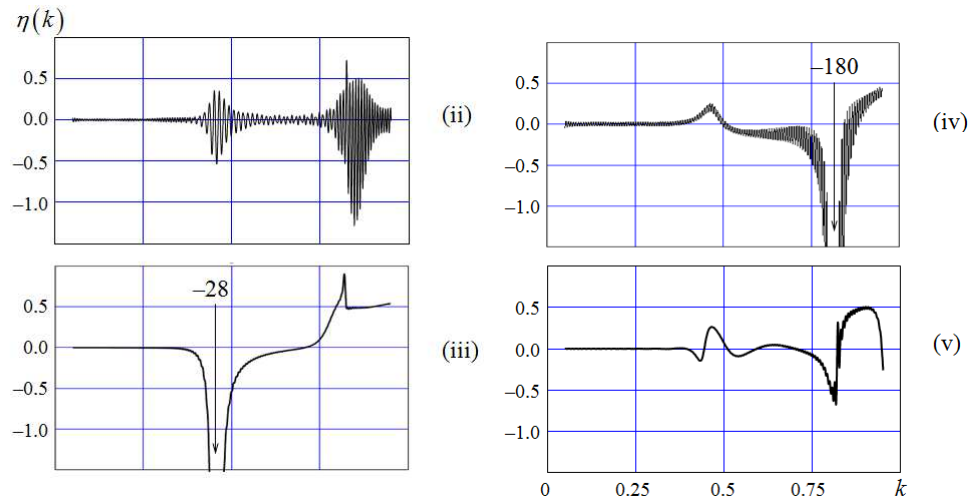
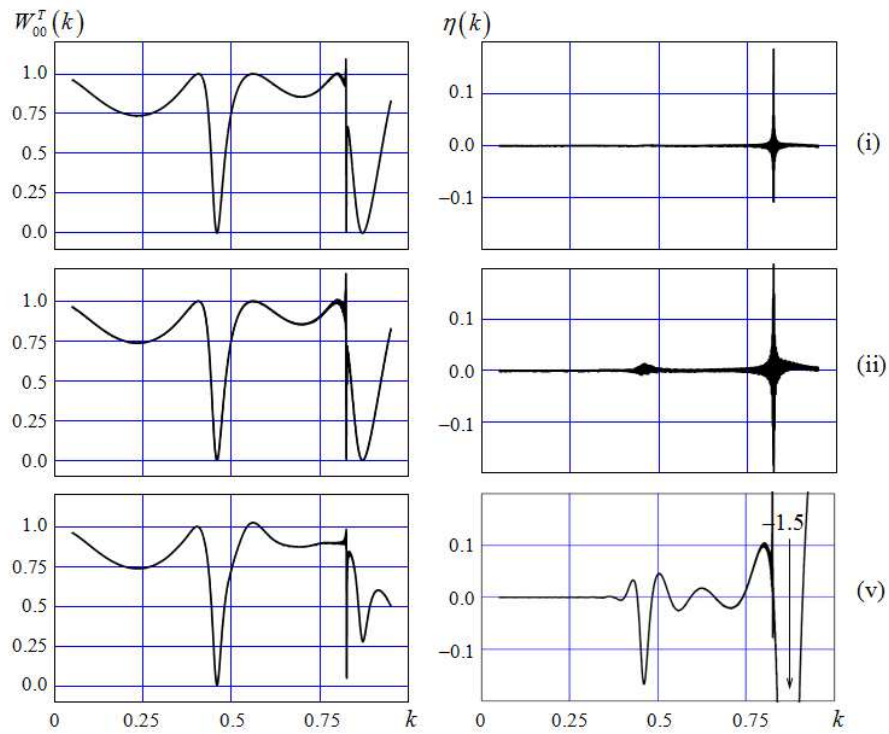**FIG. 8:** Function $\eta(k)$ computed using conditions (ii)–(v)

FIG. 9: Functions $W_{00}^{T}(k)$ and $\eta(k)$ computed using conditions (i), (ii), and (v)

Thus, only two out of five tested absorbing conditions are suitable for further numerical experiments with significant influence of weakly decaying eigenoscillations.

These are nonlocal EAC (i) and local EAC (ii). Let us extend the duration of computation to $T = 8000$ (800 000 time steps). With nonlocal EAC (i), the computational scheme remains stable, the amplitude of $U(g_1,t)$ at the end of computation is 50 times smaller than at the end of excitation, Fig. 10(a). The maximum discrepancy level $\eta(k)$ is reduced to 0.01, which corresponds to the maximum relative error of 1% in the determination of $W_{00}^T(k)$ and $W_{00}^R(k)$, Fig. 10(b). The same result could be also obtained with local EAC (ii) ($M = 5000$ for $T = 8000$). But in order to maintain the stability of the computational scheme with local EAC (ii), it is necessary to increase M with increasing T.
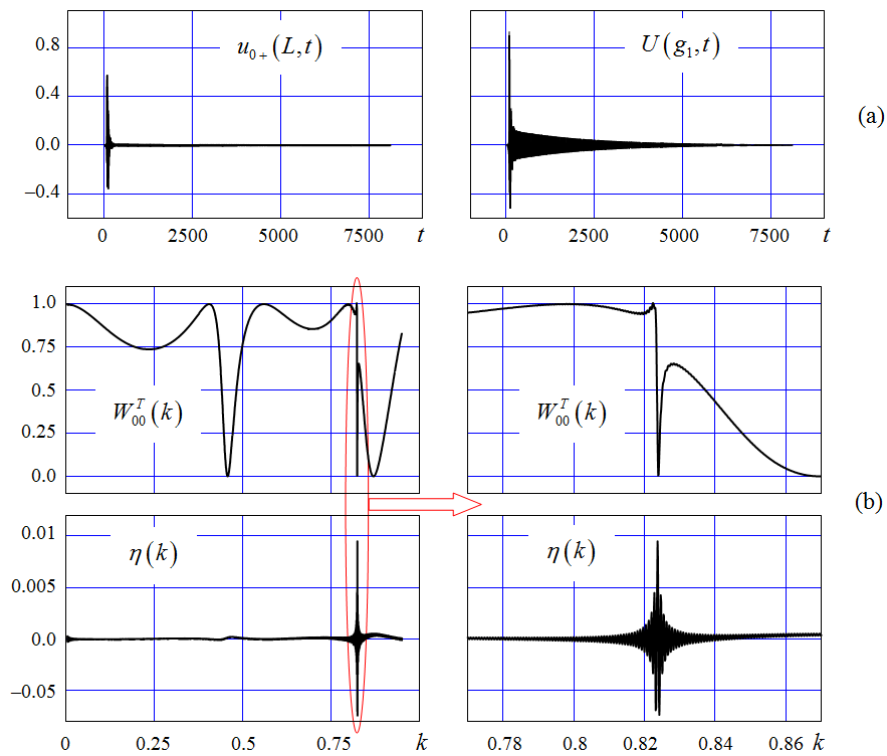

FIG. 10: Functions Hard test of condition (i): (a) Time-domain characteristics; (b) Frequency-domain characteristics

7. CONCLUSIONS

The type of absorbing conditions being used significantly affects the properties of computational schemes for solving electromagnetic initial boundary value problems, and the quality of numerical results obtained with their help. It is important for absorbing conditions to retain the classes of correctness of open problems when they

are replaced with closed ones, do not violate the stability and convergence of computational schemes, and ensure the predictable accuracy of final results. For gratings and waveguides problems, local and nonlocal EACs fully satisfy these requirements. EACs turn original open problems into equivalent closed ones [16,22] and therefore do not distort the physics of processes under study. Under the conditions of possible resonant wave scattering, only EACs can provide accurate numerical solutions, which approximate exact solutions good enough.

REFERENCES

1. Taflove, A. and Hagness, S.C., (2000) *Computational Electrodynamics: The Finite-Difference Time-Domain Method*, Boston: Artech House.
2. Engquist, E. and Majda, A., (1977) Absorbing boundary conditions for the numerical simulation of waves, *Math. Comput.*, **31**(139), pp. 629-651.
3. Mur, G., (1981) Absorbing boundary conditions for the finite difference approximation of the time-domain electromagnetic-field equations, *IEEE Trans. EMC*, **23**(4), pp. 377-382.
4. Tirkas, P.A., Balanis, C.A., and Renaut, R.A., (1992) Higher order absorbing boundary conditions for FDTD-method, *IEEE Trans. Antennas Propag.*, **40**(10), pp. 1215-1222.
5. Mei, K.K. and Fang, J., (1992) Superabsorbtion – a method to improve absorbing boundary conditions, *IEEE Trans. Antennas Propag.*, **40**(9), pp. 1001-1010.
6. Berenger, J.-P., (1994) A perfectly matched layer for the absorption of electromagnetic waves, *J. Comput. Phys.*, **114**(1), pp. 185-200.
7. Berenger, J.-P., (1996) Three-dimensional perfectly matched layer for absorption of electromagnetic waves, *J. Comput. Phys.*, **127**(2), pp. 363-379.
8. Sacks, Z.S., Kingsland, D.M., Lee, R., and Lee, J.F. (1995) A perfectly matched anisotropic absorber for use as an absorbing boundary condition, *IEEE Trans. Antennas Propag.*, **43**(12), pp. 1460-1463.
9. Maikov, A., Sveshnikov, A., and Yakunin, S., (1986) Difference scheme for transient Maxwell equations in waveguide systems, *J. Comput. Math. Math. Phys.*, **26**(3), pp. 851-863, (in Russian).
10. Perov, A.O., Sirenko, Y.K., and Yashina, N.P, (1999) Explicit conditions for virtual boundaries in initial boundary value problems in the theory of wave scattering, *J. Electromag. Waves Appl.*, **13**(10), pp. 1343-1371.
11. Sirenko, Y.K, (2002) Exact absorbing conditions in outer initial boundary-value problems of the electrodynamics of nonsinusoidal waves. Part 2: Waveguide units and periodic structures, *Telecommunications and Radio Engineering*, **57**(12), pp. 1-31.
12. Sirenko, K.Y. and Sirenko, Y.K., (2005) Exact absorbing conditions in the initial boundary-value problems of the theory of open waveguide resonators, *Comput. Math. Math. Phys.*, **45**(3), pp. 490-506.
13. Sirenko, Y.K., Strom, S., and Yashina, N.P., (2007) *Modeling and Analysis of Transient Processes in Open Resonant Structures. New Methods and Techniques*, New York: Springer.
14. Sirenko K.Y., Sirenko Y.K., and Yashina N.P., (2010) Modeling and analysis of transients in periodic gratings. I. Fully absorbing boundaries for 2-D open problems Resonant wave scattering, *J. Opt. Soc. Am. A*, **27**(3), pp. 532-543.
15. Sirenko, Y.K. and Strom, S. (eds), (2010) *Modern Theory of Gratings. Resonant Scattering: Analysis Techniques and Phenomena*, New York: Springer.
16. Sirenko, K., Pazynin, V., Sirenko, Y., and Bagci, H., (2011) An FFT-accelerated FDTD scheme with exact absorbing conditions for characterizing axially symmetric resonant structures, *Progress Electromagn. Res.*, **111**, pp. 331-364.
17. Sirenko, Y.K. and Velychko, L.G. (eds.), (2016) *Electromagnetic Waves in Complex Systems*, New York: Springer.

18. Kravchenko, V.F., Sirenko, Y.K., and Sirenko, K.Y., (2011) *Electromagnetic Wave Transformation and Radiation by Open Resonant Structures*, Moscow, Russia: Fizmathlit, (in Russian).

19. Sirenko K.Y., Sirenko Y.K., and Yashina N.P., (2010) Modeling and analysis of transients in periodic gratings. II. Resonant wave scattering, *J. Opt. Soc. Am. A*, **27**(3), pp. 544-552.

20. Sirenko, Y.K. and Velychko, L.G., (2009) Controlled changes in spectra of open quasi-optical resonators, *Progress Electromagn. Res. B*, **16**, pp. 85-105.

21. Sirenko, Y.K., Velychko, L.G., and Erden, F., (2004) Time-domain and frequency-domain methods combined in the study of open resonance structures of complex geometry, *Progress Electromagn. Res.*, **44**, pp. 57-79.

22. Velychko, L.G., Sirenko, Y.K., and Velychko, O.S., (2006) Time-domain analysis of open resonators. Analytical grounds, *Progress Electromagn. Res.*, **61**, pp. 1-26.

23. Shafalyuk, O., Smith, P., and Velychko, L.G., (2012) Rigorous substantiation of the method of exact absorbing conditions in time-domain analysis of open electrodynamic structures, *Progress Electromagn. Res. B*, **41**, pp. 231-249.